Al-Azhar Engineering 16th International Conference

Vol. 19, No. 72, July 2024, 75 - 91

ACTIVE COOLING HEAT TRANSFER COEFFICIENT ENHANCEMENTS IN POROUS COMPACT HEAT EXCHANGER

Ramy Farid[1]*, W. Aboelsoud[2], Said M.A. Ibrahim[1]

[1]Mechanical Engineering Department, Faculty of Engineering, Al-Azhar University, Cairo, Egypt

[2]Mechanical Power Engineering Department, Faculty of Engineering, Ain Shams University, Cairo, Egypt

***Correspondence:** ramyfareed.18@azhar.edu.eg

Citation:

R. Farid, W. Aboelsoud, S.M.A. Ibrahim "Active Cooling Heat Transfer Coefficient Enhancements in Porous Compact Heat Exchanger", Journal of Al-Azhar University Engineering Sector, vol. 19, pp. 75 - 91, 2024.

Received: 16 November 2023

Revised: 24 December 2023

Accepted: 02 January 2024

DOI:10.21608/auej.2024.249276.1476

ABSTRACT

Due to the poor thermal properties of the air and the resistance of the boundary layer, enhancing the heat transfer coefficient HTC is a challenging problem. In this study, the hydro-thermal characteristics of V-shape copper porous media attached to a vertical heat source were studied by using the active cooling forced convection technique. The performance of hydraulic is expressed by pressure drop through the porous insert material while the thermal performance is expressed by the overall HTC and Nusselt number. To conduct this research the finite element method (FEM) is used by employing the COMSOL software. The V-shape geometry was chosen as the porous thickness is 2 mm and the porous height is 4 mm. The V-shape angle was changed from 14 to 180, and the airflow velocity was varied from 0.7 m/s to 3 m/s. The results show that angle 14 gives the minimum pressure drop so minimum pumping power. For laminar airflow changing air velocity from 0.7 to 3 m/s led to a change in the pressure drop from 44 to 530 Pa and the Nusselt number ranges from 186-1592. V-shape with an angle of 14 degrees gives the best hydraulic performance for the selected geometry and The best performance criteria is at porosity 25% and Reynolds number 4617. The best enhancement of the heat transfer coefficient from this geometry is 8 times more than that from the bare model. Correlations for Nusselt number and performance criteria were concluded.

KEYWORDS: Active cooling, Porous materials, Heat exchanger, Effectiveness, Heat transfer coefficient. Forced convection.

تعظيم معامل انتقال الحراره عن طريق الحمل القسري في مبادلات حرارية ايجابية

رامي فريد[1]*، وليد ابوالسعود[2]، سعيد محمد على ابراهيم[1]

[1]قسم الهندسة الميكانيكية- كلية الهندسة- جامعة الأزهر- مدينة نصر 11884، القاهرة، مصر

[2]قسم هندسة القوى الميكانيكية- كلية الهندسة- جامعة عين شمس، القاهرة مصر

***البريد الاليكتروني للباحث الرئيسي :** ramyfareed.18@azhar.edu.eg

الملخص

نظرًا للخصائص الحرارية الضعيفة للهواء والمقاومة الحرارية العالية للطبقة الجدارية، فإن تعزيز معامل نقل الحرارة يمثل مشكلة صعبة. في هذه الدراسة تمت دراسة الخصائص الهيدروليكية والحرارية للوسائط المسامية النحاسية على شكل حرف V والمتصلة

بمصدر حرارة رأسي باستخدام تقنية الحمل القسري بالتبريد النشط. يتم تقييم الأداء الهيدروليكي من خلال انخفاض الضغط من خلال المادة المسامية بينما يتم تقييم الأداء الحراري من خلال رقم معامل انتقال الحراره بالحمل القسري ورقم نسلت الإجمالي. تم استخدام طريقة التحليل العددية لإجراء هذا البحث من خلال استخدام برنامج كومسيل. تم اختيار الشكل الهندسي على شكل V حيث يبلغ سمك المادة المسامية 2 مم وارتفاعها 4 مم. تم تغيير زاوية الشكل V من 14 إلى 180 درجة، وتم تغيير سرعة تدفق الهواء من 0.7 م/ث إلى 3 م/ث. أظهرت النتائج أن الزاوية 14 تعطي الحد الأدنى من انخفاض الضغط وبالتالي الحد الأدنى من قوة الضخ اللازمة لتحريك الهواء. بالنسبة لتدفق الهواء بمتوسط سرعة تبلغ 0.7-3 م/ث، يتراوح انخفاض الضغط من 44-530 باسكال ويتراوح رقم نسلت من 186-1592. الشكل V بزاوية 14 درجة يعطي أفضل أداء هيدروليكي وأفضل معايير الأداء هي المسامية 25% ورقم رينولدز 4617. أفضل تحسين لمعامل انتقال الحرارة من هذ النموذج هو 8 مرات أكثر من نموذج خالي من المواد المسامية. تم التوصل إلى معادلات رياضية تربط بين عدد نسلت ومعايير الأداء.

الكلمات المفتاحية : التبريد الايجابي، المواد المسامية، المبادل الحراري، الفعالية، معامل انتقال الحرارة، الحمل القسري.

1. INTRODUCTION

Heat transfer enhancement techniques, which can be either passive, active or a combination of both, find widespread application across various engineering fields, including heat exchangers, industrial processes, evaporator systems, thermal power plants, air conditioning units, refrigeration systems, chemical reactors, radiators for spacecraft and automobiles. These techniques are crucial for improving heat transfer rates while simultaneously reducing the size and cost of equipment, especially in heat exchangers. Among these techniques, passive heat transfer methods stand out, as they utilize flow passages to boost heat transfer and offer advantages over active methods due to their compatibility with existing heat exchangers.

In the context of compact heat exchanger design, the selection of an appropriate passive insert configuration is vital, considering the specific working conditions of the heat exchanger, encompassing both flow and heat transfer requirements. Air is commonly employed in cooling applications, and the use of extended surfaces, particularly smaller effective fins, has proven effective in reducing air-side thermal resistance and enhancing heat transfer efficiency. Porous fins, characterized by their efficiency and compactness, outperform traditional rectangular cross-section fins, especially in electronic applications. Porous fins exhibit superior heat transfer capabilities compared to solid fins, making them an attractive subject for thermal analysis under forced convection conditions. In recent developments, high-porosity metal foams have found applications in aerospace structures, chemical reaction catalysis, and the construction of robust panels.

An experimental study was done to show the effect of different parameters like pore density, porous material height, and the number of porous fins, on the thermal performance of the foam heat sinks. As a result of the study, the method of fused bonding causes a reduction in the thermal contact resistance by 19 times, compared to the epoxy-gluing process. The results showed that the Nusselt number is 30% higher by using the fused bonding method compared to using the epoxy-glued method. Additionally, the heat flux from the foam heat sink was twice compared to the normal heat sink [1].

The hydro-thermal performance of forced convective heat transfer in a heat sink combining metal foam and pin fins was numerically analysed. various porosities were tested (ranging from 0.8 to 0.95) under laminar flow conditions. And deionized water was used as a working fluid. The results showed that the hybrid heat sink, benefiting from the synergistic effects of solid pin fins and metal foam, exhibited significantly improved heat transfer performance, the normal pin fin showed

an improvement of 267% and the metal foam heat sinks showed an improvement by 36%, at a Reynolds number of 1000 [2].

A numerical study was performed on a circular tube with twisted conical strip inserts fitted on the tube and the laminar flow thermal-hydro performances were tested. The results showed that the twist angle was the most effective parameter on both the friction factor and Nusselt number [3].

[4-8] Studies were carried out on metal foam heat exchangers to enhance their thermal and hydraulic performance, using copper foam and aluminum heat sinks.

The performance of a porous fin made of aluminum alloy 6101 compared to a normal louvered fin and normal louvered fin showed better performance [9].

An experimental and numerical studies on the hydraulic performance corrugated porous heat exchanger. It was concluded that if the dynamic viscosity increased the flow distribution was improved but the pressure drop was increased. A correlation between Reynolds number and the pressure drop was conducted [10].

A numerical study evaluated the hydraulic and thermal performances of tube channels was partially filled with grooved metal foams under laminar steady flow conditions with constant heat flux. Two pitches of helical grooves with a diameter ratio of 0.5 resulted in a reduction in pumping power by approximately 17% [11].

The thermal and hydraulic performances of a heated vertical flat plate heat exchanger with three brass wire mesh materials of different porosities were investigated, showing that increasing porosity led to an enhancement in the rate of heat transfer and decreased the pressure drop [12].

A numerical study examined the thermal and hydraulic performances of three different heat exchangers, including a metal foam baffle heat exchanger, a non-baffle heat exchanger, and a combination of metal foam baffle and fin heat exchanger. The results showed that metal foam baffle heat exchanger achieved up to about a 584% increase in heat transfer rate [13].

An experimental study was performed to evaluate the performance of an annular porous fin rounded in a vertical cylinder by using natural convection. The results indicated that the average Nusselt number was dependent on permeability, the heat transfer enhancement was 8% using one fin and the maximum achievement was 131% with a porous fin layer [14].

In natural convection, the effects of porous material were studied using a nano-fluid inside a triangular chamber. It was concluded that the rate of heat transfer was affected by using a hybrid nano-fluid (water/aluminum and oxide-copper) inside a porous material [15].

In the case of porous flat plate fins placed in a vertical heat source under natural convection, the heat transfer rate from the porous fin could exceed that of a solid fin. Additionally, it was observed that increasing the fin length and effective thermal conductivity improved heat transfer up to a certain limit, with no further enhancement beyond those parameters [16].

A natural convection study around a horizontal solid cylinder wrapped with porous material was conducted to identify optimal conditions for thermal insulation or improving heat transfer rates. It was found that a Darcy number limit needed to be considered, and to achieve this, high thermal conductivity porous media, and high permeability should be used [17].

A hybrid nano-fluid of water/aluminum copper oxide inside a porous enclosure with differential heating on its upright walls was studied in natural convection. Using glass balls as nanoparticles and aluminum foam as the porous material reduces the mean Nusselt numbers and

increasing the nanoparticle volume fraction led to a decrease in the heat transfer rates when increasing the nanoparticle volume fraction [18].

An experimental study of forced convection heat transfer was performed on a circular tube filled with a metal foam with nanofluid flow. It was concluded that there was an improvement in the rate of heat transfer along with an increase in the pressure drop. A correlation between Nusselt number and nano-fluid volume fraction was identified [19].

It was numerically shown that adding nanoparticles to a fully developed laminar by using mixed convection including forced and natural convections of water in an annulus-reinforced secondary flow [20].

The study of natural convection between two eccentric cylinders revealed that reducing the Lewis number resulted in fewer nanoparticle collisions and a decrease in the Nusselt number [21].

The primary aim of this study is to conduct a comprehensive numerical analysis of the hydraulic and thermal performance associated with a compact V-shape porous insert applied to a vertical heat source, with the ultimate goal of enhancing heat transfer rates. The investigation involves the examination of multiple heat exchanger geometries, all incorporating copper foam porous material with varying porosities. The objective is to identify the optimal geometry for the porous material within the compact heat exchanger that delivers superior hydraulic and thermal performance.

2. The heat exchanger geometry

The heat exchanger's geometry, as depicted in **Figure 1**, involves the flow of air over a vertical heat source characterized by dimensions (L x W) and a specific height (H). Within this setup, the heat transfer medium is a V-shaped copper foam. The key parameters under investigation for this medium are the effective thickness (t), the V-shape angle (θ), and the porosity (Ɛ). The focus of this research is passive cooling heat transfer utilizing the porous medium, particularly in the context of laminar airflow. It's important to note that this specific shape serves as a modular unit that can be replicated to create the desired overall heat exchanger geometry [21].

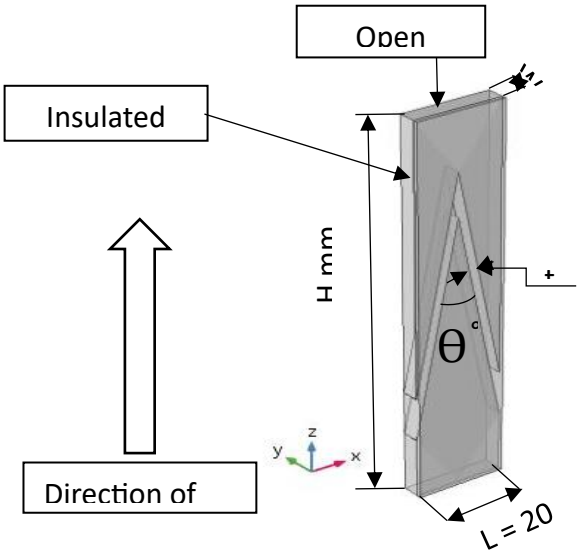

Figure 1. Computational domain.

3. Numerical Model

The domain is divided into two distinct regions, as illustrated in **Figure 1**. The first region is the free airflow domain, comprising an empty channel filled with air, while the second region is the porous matrix domain, where the porous material is located, and air occupies the pores within the matrix. The solve was for the temperature, velocity and pressure fields within the computational domain, the Finite Element Method (FEM) was applied. This numerical analysis was conducted using COMSOL Multi-Physics software [22].

3.1 Assumptions

Some assumptions are made for the present model calculations:

- Porous attachments are assumed to be homogeneous and isotropic and the porosity of copper foam, thickness, and permeability are uniform .
- Because of the temperature difference is only 2 ^{0}C the radiation heat transfer is too small so it can be neglected.
- The copper foam porous permeability is taken as $10 * 10^{-10}\ \ darcy\ unit\ (m^2)$ [4]

3.2 Mesh dependence test

To choose the best mesh size, coarse, normal and fine sizes were evaluated to find out the effect of mesh size on the bulk temperature (T_{bulk}). The evaluation gave a difference in temperature of only 0.02 °C so the variation and error percentage is only 0.0061 % between coarse and fine meshes, therefore a coarse mesh size was chosen for all test runs. This saves hours in the time of test runs which are many. **Figure 2** shows the effect of mesh size on the bulk temperature of air flow.

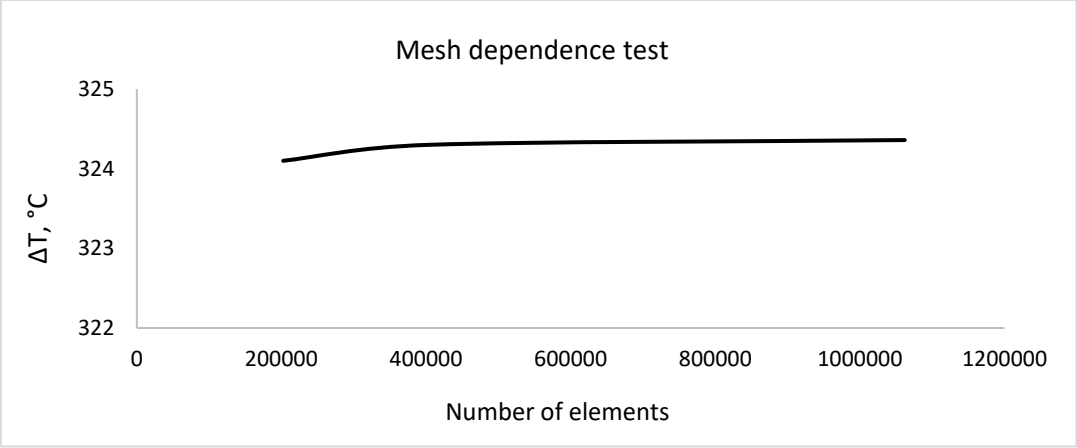

Figure 2. Mesh dependence test

3.3 Boundary Conditions

The boundary conditions such as the velocity and the inlet temperature of the air are listed in **Table 1**. The symmetry of the geometry results is reduction in the computational time, because of the reduced number of variables.

Table 1 Boundary conditions.

Boundary	Parameter	Value
Inlet	Air velocity V_a	0.7- 3 m/s
Exit	Gage Pressure	0
Wall	Velocity	0
Symmetry	∇v.n = 0	0
Temperature	Inlet air temperature	293 K
Outflow	n. ∇T	0
Thermal insulation	n. ∇T	0
Heat flux	$\dot{q}$	5000 W/m^2

3.4 Forced airflow

3.4.1 Continuity equation

Within the computational domain, a steady laminar airflow is established. The forced convection air velocity at the inlet varies from 0.7 to 3 m/s. It's important to note that air density varies with temperature and pressure, and these variables change with position (x, y, z). The continuity equation is employed to account for these variations in the system [15].

$$\nabla.(\rho v) = 0 \quad (1)$$

In this analysis, the air is treated as a Newtonian fluid, and it's assumed that the air is not subjected to any forces. Additionally, the dynamic viscosity of the air is considered as a function of temperature, and this viscosity value varies with position within the computational domain [15].

$$\rho(v.\nabla)v = \nabla.\left[-p + \mu(\nabla v + (\nabla v)^T) - \frac{2}{3}\mu(\nabla v)I\right] \quad (2)$$

Where μ is the air kinematic viscosity (m^2/s), and p is the air outlet pressure Pa (N/m^2).

3.4.3 Energy equation

The thermal conductivity is considered to be a temperature-dependent [15].

$$\rho c_p v.\nabla T = \nabla.(k\nabla T) \quad (3)$$

3.5 Model Validation

The Finite Element Method (FEM) was employed to solve the velocity, pressure, and temperature fields in the computational domain using COMSOL Multi-Physics software, the inputs are heat flux, ambient temperature, and pressure, the outputs are bulk temperature and the surface temperature. Nusselt number (Nu) can be calculated from equation (10) and Rayleigh number (Ra) from the following equation

$$Ra = \frac{\rho^2.g.\beta.\Delta T.Lc^3}{\mu^2} \quad (4)$$

Where g is the gravitational acceleration, $\frac{m^2}{s}$, ρ is air density, $\frac{kg}{m^3}$, β is the coefficient of thermal expansion = $\frac{1}{T_a}$, where T_a is ambient temperature, K, Lc is characteristic length, m, and μ is the dynamic viscosity, $\frac{kg}{m.s}$.

The model validation was done at free convection and was confirmed by plotting the relation between Nusselt (Nu) and Rayleigh (Ra) numbers for a bare vertical wall without any porous medium inside, and the results are compared with those obtained from equation (5) [23] which is valid for vertical bare heat source.

$$Nu = \frac{Ra^{1/3}}{[9.742 - 0.1869 \ln (Ra)]^{4/3}} \quad (5)$$

The comparative validation results are presented in **Figure 3.** Good agreement is shown between the present model and equation (5).

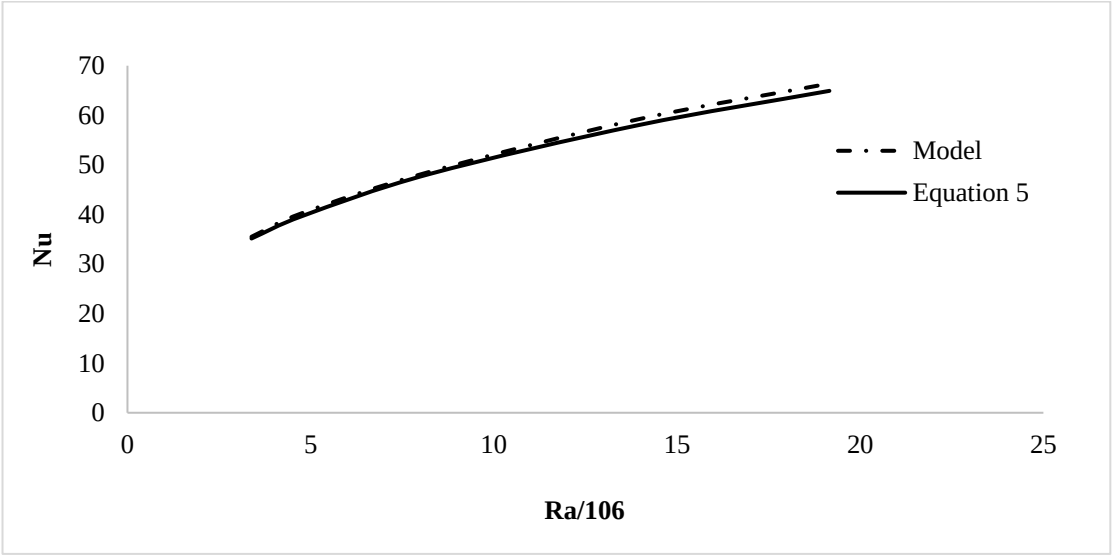

Figure 3. Model validation

3.6 Porous matrix

The porous matrix domain which accommodates the porous material with air occupying the pores.

3.6.1 Continuity equation

The air velocity in the porous matrix is called filtration velocity (v_f). The air density is pressure and temperature-dependent [15].

$$\nabla . (\rho v_f) = 0 \quad (6)$$

Where the v_f is the flow velocity (m/s).

3.6.2 Momentum equation

Within porous media, the flow behavior is described by the Brinkman–Forchheimer-extended Darcy equation [15]. The pressure drop, as governed by Darcy's law, is combined with

the Forchheimer drag term to formulate the momentum equation, taking into account the porous characteristics of the medium.[15]

$$\frac{\rho}{\varepsilon}(v_f.\nabla)\frac{v_f}{\varepsilon} = \nabla.\left[-p + \frac{\mu}{\varepsilon}(\nabla v_f + (\nabla v_f)^T) - \frac{2}{3}\frac{\mu}{\varepsilon}(\nabla v_f)I\right] - \frac{\mu}{k}v_f - \beta_f {v_f}^2$$

(7) Where β_f is the Forchheimer coefficient (kg/m^4) and $= \frac{\rho C_f}{\sqrt{k}}$, and ε is the porosity.

3.6.3 Energy equation

Steady flow was considered and no heat generation in the porous media [15].

$$c_p V_f.\nabla T = \nabla.(K_{eff}\nabla T) \quad (8)$$

3.7 Solution Procedure and model explanation

Using COMSOL Multiphysics software, Navier- Stokes equations were solved using the finite element method. Starting with the continuity and momentum equations in free convection at roam remperature of 293 K and air velocity zero, using a coarse, normal and fine mesh element.

The results of the velocity and the pressure fields were optained by solving the energy equation in conjunction with the continuity and momentum equations, and the mass flow rate and bulk temperature were optained. The convergence was considered when the max relative tolerance of 10^{-10} is attained. **Table 2** showing the elemnets size parameter and quality.

Table 2 Elements size parameters.

	coarse	normal	fine
Tbulk	324.38	324.37	324.36
time of the run	14 min	40 min	1.30 hr
no. of elem.	202408	403064	1062049
quality	0.1979	0.0687	0.1751

4. Results and Discussion

This work studied the effect of the heat exchanger geometry on its heat transfer characteristics. The studied parameters were the porous medium thickness and height, the V-angel of the medium, and its porosity. The performance of the heat exchanger is evaluated through the volumetric HTC, Performance Evaluation Criteria (PEC), pumping power, and pressure drop.

4.1 Forced Convection

The efficiency of heat removal in a heat sink, under constant conditions like geometry, air velocity, and heat transfer amount, is reflected by the base temperature of the heat sink at a given inlet air temperature. A smaller difference between base temperature (T_b) and inlet temperature (T_{ai}) results in a higher HTC, and it can be expressed as follows.

$$HTC = \frac{Q}{A(T_b - T_{a,i})} \quad (9)$$

Then, the Nusselt number is

$$\mathrm{Nu} = \frac{\mathrm{HTC}.\,\mathrm{L}_c}{\mathrm{k}_a} \tag{10}$$

Where, L_c is the characteristic length of the channel which is the height of the heat source, and k_a is the thermal conductivity of the air at mean film temperature for the natural convection model. The heat transfer rate is denoted by

$$\dot{\mathrm{Q}} = \dot{\mathrm{m}}.\,\mathrm{c}_{\mathrm{p,a}}.\,(\mathrm{T}_{\mathrm{a,o}} - \mathrm{T}_{\mathrm{a,i}}) \tag{11}$$

The air mass flow rate is

$$\dot{\mathrm{m}} = \iint \rho.\,\mathrm{v}.\,\mathrm{dA} \tag{12}$$

The bulk temperature was generally used to calculate the air outlet temperature and is given by

$$\mathrm{T}_{\mathrm{bulk}} = \frac{1}{\dot{\mathrm{m}}.\mathrm{c}_{\mathrm{p,a}}} \iint \rho.\,\mathrm{c}_{\mathrm{p,a}}.\,\mathrm{T}.\,\mathrm{v}.\,\mathrm{dA} \tag{13}$$

4.2 Comparison between passive and active cooling to choose the best porous insert height

Figure 4 shows the effect of porous insert height on the effectiveness of forced and free convection at a porosity of 75%. These results confirm the correct choice of porous insert of 4 mm for both passive and active convection modes. Increasing the height affecting the effectiveness of the fin and at certain height the effectiveness decreases a lot so adding more material is waste of material so optimum effectiveness was at 4 mm fin Height.

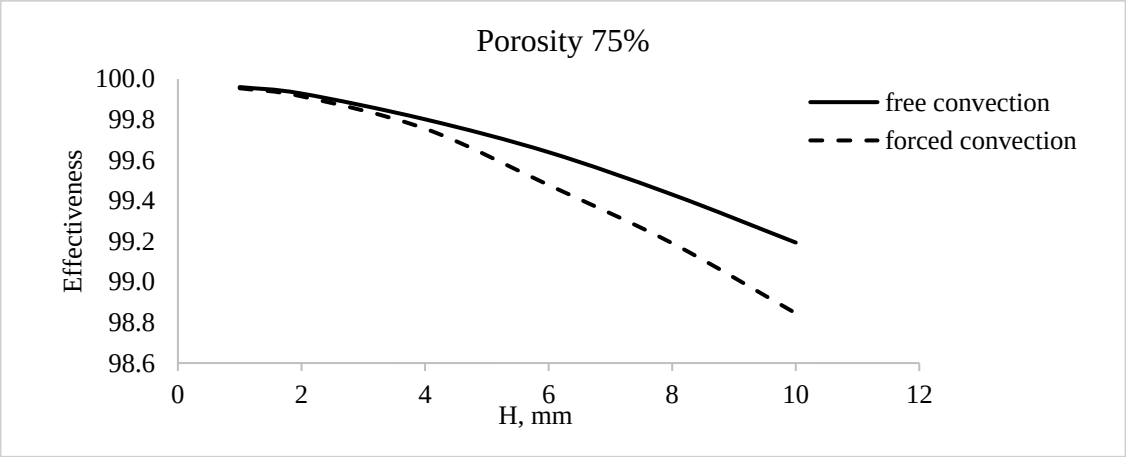

Figure 4. Effect of the fin insert height on the effectiveness, for forced and free convection.

Figure 5 Represents the effect of V-shape angels from 14^0-180^0 on the pressure drop across the porous medium. The smallest angle of 14^0 is that which makes the porous insert fits the channel. The results depict that the minimum pressure drop at this minimum angle, and consequently a minimum pumping power.

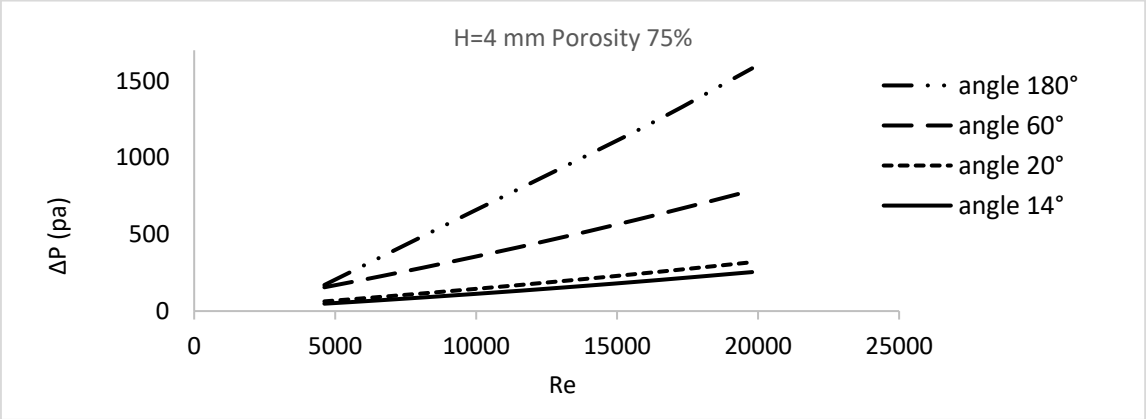

Figure 5. Effect of V-shape angel on the pressure drop.

To further confirm the best geometry, another comparison was employed to show the effect of angle, θ on Nusselt number enhancement ratio with Reynolds number. Inserting porous media can heighten the heat transfer rate greatly compared to the bare model. The largest increase in Nusselt number is 3.5 times that of the bare model as reported in **Table 3.** All results indicate that the thermal performance (as measured by Nusselt number and Renolds number) for all angles is the same, but the angle that produces the least pressure drop is 14 degrees. So that the V-shape angle is chosen to be 14 degrees.

Table 3. Effect of V-shape angle on Nusselt number.

Porosity,	Re	Nu/Nu bare			
		Angle, θ^0			
		180	60	20	14
75 %	0.7	3.52	3.53	3.53	3.53
	1	2.76	2.76	2.76	2.76
	1.5	2.15	2.15	2.15	2.15
	2	1.86	1.86	1.86	1.86
	2.5	1.69	1.69	1.69	1.69
	3	1.59	1.59	1.59	1.59

Figure 6 represents the variation of Nusselt number against Reynolds number at different porosities All results show heat transfer enhancement over that for the bare model. The maximum enhancement was achieved with porosity of 25% and at Renolds number close to 2*10^4. Furthermore, an empirical correlation was found (by using MATLAB software) for the porous medium in terms of Nusselt number, Reynolds number, and the porosity as

$$Nu = 40.85 * Re^{0.2692} * \varepsilon^{-0.7783} \quad (14)$$

Valid for $4617 \leq Re \leq 19789$

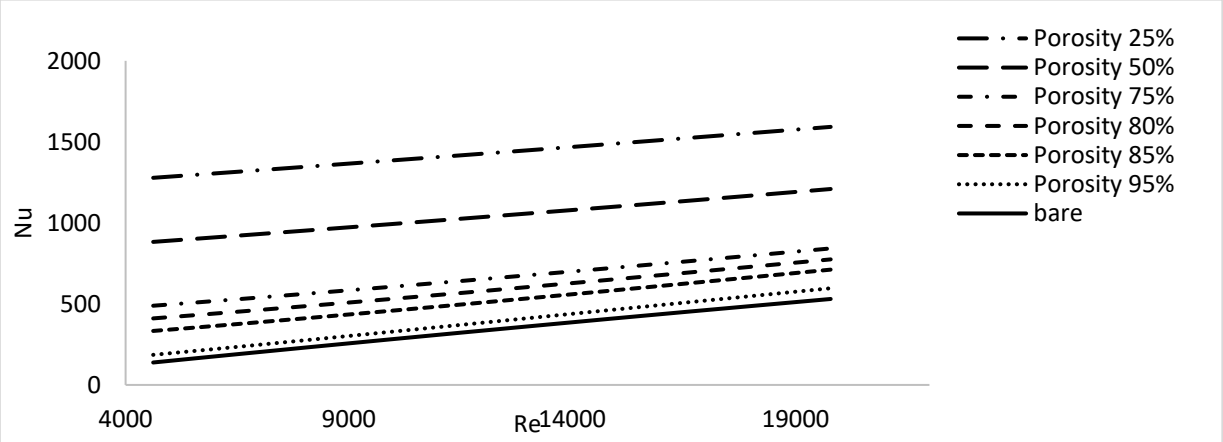

Figure 6. Nusselt number variation with Reynolds number.

Nusselt number enhancement ratio is the relation between Nusselt number for the model compared with the Nusselt number of the bare model without the porous insert, so it gives a direct indication about the increase of the Nusselt number compared with the bare model so as heat transfer coefficient. **Figure 7** displays the variation of the Nusselt number enhancement ratio with Reynolds number for different porosities. Inserting porous media can heighten the heat transfer rate greatly compared to the bare model. The largest increase in Nusselt number is higher than 8 times at porosity of 25%, while the minimum increase was for the porosity of 95%, where it is close to the bare heat source at a low Reynolds number. For higher Reynolds number, all porosities give very close achievements in the heat transfer enhancement and the maximum increase is 3 times than the bare heat source.

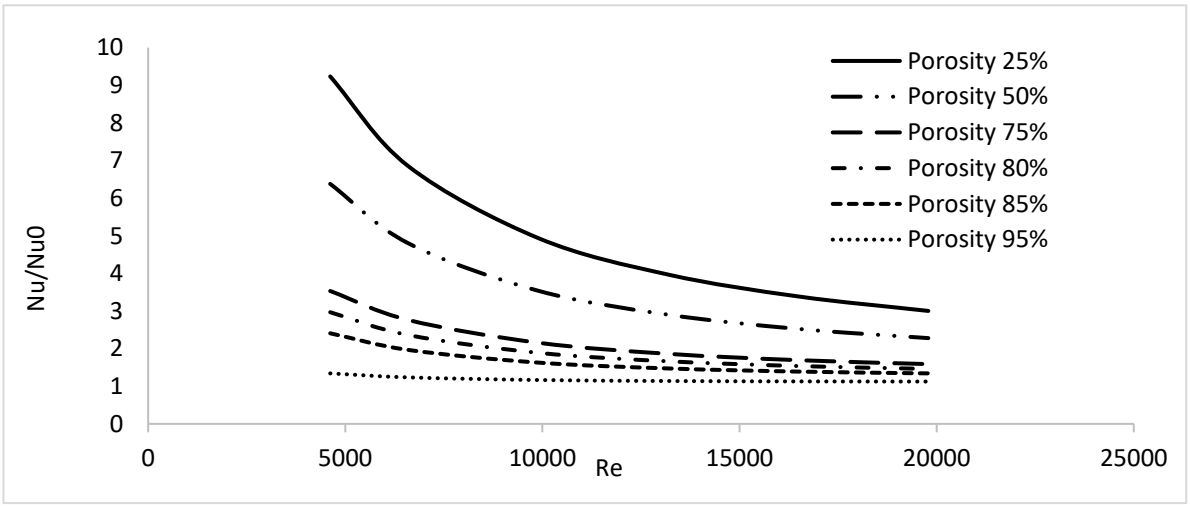

Figure 7. Nusselt number enhancement ratio with Reynolds number.

To represent the hydraulic performance, the pressure drop data for all models, ΔP is made dimensionless in the form of Euler number (Kp,∞) as it displayed in equation 15. The variation of

Euler number with Reynolds number is represented in **Figure 8**. The results shows that at small Reynolds numbers the difference in pressure drop represented in Euler number is showing a big difference at different porosities and the porosity of 25% gives the highest Euler and pressure drop. Increasing Reynolds number results in decreasing Euler number so pressure drop. At high Reynolds Numbers the porosity does not show a big effect on the pressure drop.

$$K_{p,\infty} = \frac{\Delta P}{\frac{1}{2}*\rho*v^2} \quad (15)$$

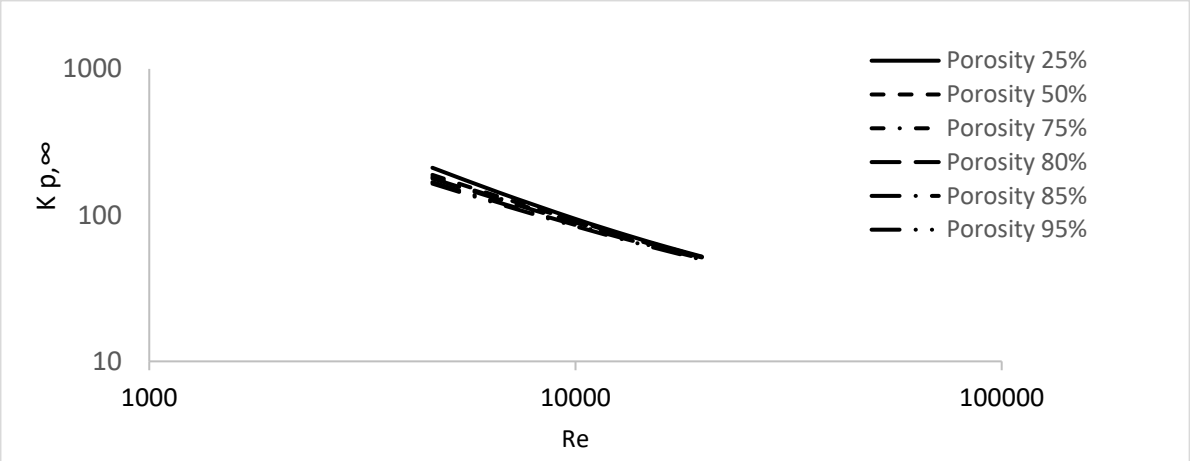

Figure 8. The variation of Euler number with Reynolds number.

An empirical correlation was developed from numerical data for each porosity to demonstrate the relationship between Euler number and Reynolds number. a and b are coefficients and presented in Table 4. for equation 16.

$$K_{p,\infty} = a * Re^b \quad (16)$$

Table 4. Correlation coefficients of equation 14 for different porosities.

Porosity	25%	50%	75%	80%	85%	95%
a	168166	179974	240620	276393	337478	685186
b	-0.824	-0.829	-0.856	-0.87	-0.89	-0.962

From equation 16 Euler number $K_{p,\infty}$ is inversely proportional to Reynolds number. This proves that the flow through the porous media is laminar. The primary purpose of employing a porous matrix is to improve heat transfer coefficient. Nevertheless, the pressure drop or pumping power increases accordingly. So, various criteria for the combined hydro-thermal performance have been proposed in the literature. One is to define the volumetric heat transfer coefficient (h_v), as well as the volumetric pumping power (P/V), as described in equations 15 and 16, respectively.

$$h_v = \frac{h_o*A_o}{V} \quad (17)$$

$$P/V = \frac{\dot{V} * \Delta P}{V} \quad (18)$$

Where V is geometry gross volume and A_o is the heat transfer area of the heat source.

Figure 9. represents the relation between the volumetric heat transfer coefficient and the pumping power of the air flow at different porosities. The results show that the outer volumetric heat transfer coefficient always rises with the pumping power for active cooling.

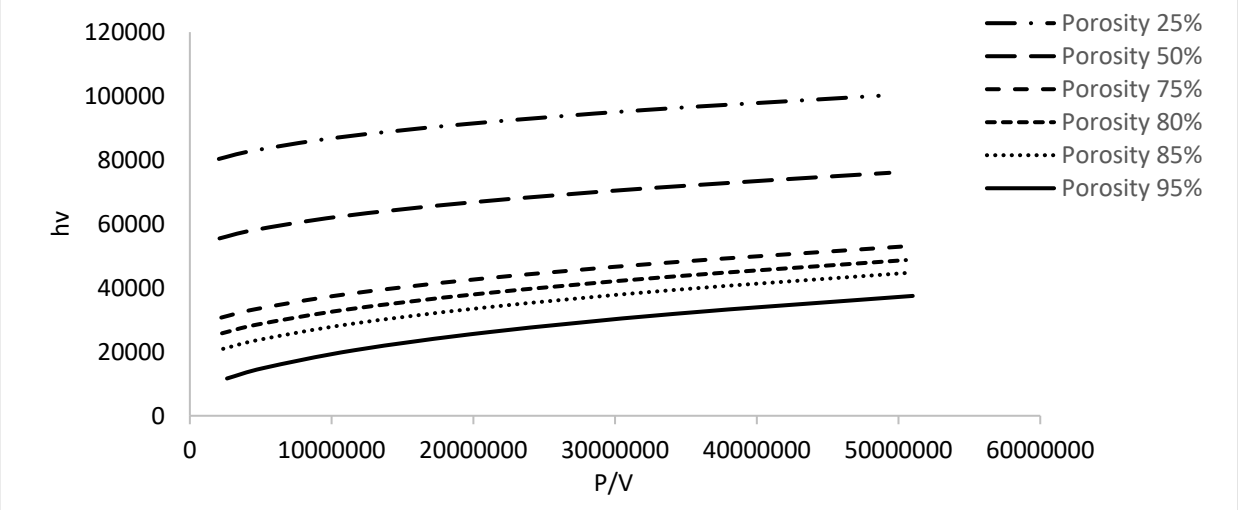

Figure 9. Relation between volumetric heat transfer coefficient and the volumetric pumping power.

A criterion for the combined hydro-thermal performance that has been proposed in the literature is the Performance Evaluation Criteria (PEC). This criteria represents the overall thermal and hydraulic performance for the same Reynolds number and is given by [2,3]

$$PEC = \frac{Nu/Nu_b}{f/f_{bare}} \quad (19)$$

Where Nu/Nu_b is the ratio between the Nusselt number for the enhanced heat exchanger and the Nusselt number for the smooth bare heat source and f/f_{bare} is also the ratio for the friction coefficient for the enhanced and the bare heat source.

Figure 10 exhibits the variation of PEC versus Reynolds number for different porosities. The results reveal that increasing the Reynolds number via increasing the air velocity, decreases the performance evaluation criteria. The porosity of 95% shows the lowest performance and 25% gives the best performance. The best performance is at the lowest Reynolds number and porosity of 25%.

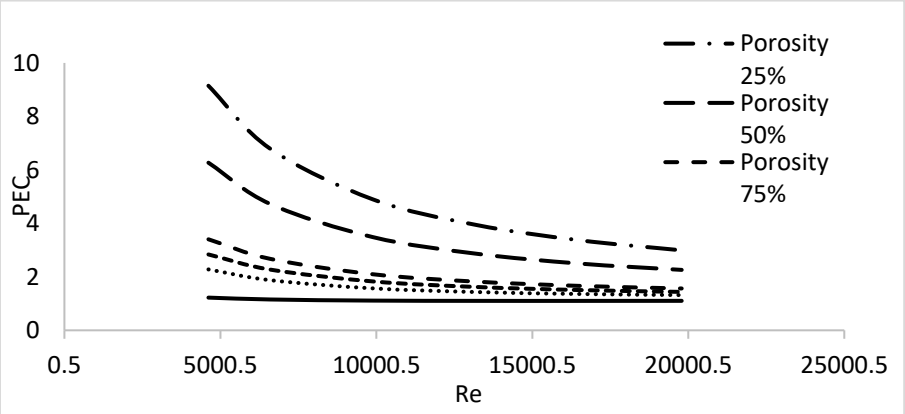

Figure 10. Variation Performance Evaluation Criteria (PEC) with Reynolds number.

Another correlation was developed from **Figure 10**, for the PEC by using Matlab software, this gives a direct indication for the designer about the best overall performance for a heat exchanger at a given Reynolds number and porosity.

$$PEC = 856.4 * \varepsilon^{-0.9136} * Re^{-0.6896} \quad (20)$$

Conclusions

In the present study, the thermal and hydraulic performance of passive cooling heat exchangers with copper foam porous material was numerically investigated. The heat source is vertical, and variations in the porous medium thickness and its v-angles, and the height of the heat exchanger were simulated using COMSOL MULTI-PHYSICS. Steady-state laminar flow was modeled. The following conclusions are obtained:

-The porous insert height affects the effectiveness and 4 mm is appropriate, since the effectiveness decreases afterward, and above 4 mm is material waste.

-A correlation was developed for the simulated porous media heat exchanger models, which presented the dependency of the Nusselt number on the porous media heat exchanger porosity and Reynolds number.

This equation has the form presented in equation 12 and is valid for the Reynolds range, $4617 \leq Re \leq 19789$

-Examining different V-shape angles for evaluating the hydraulic performance concluded that the best angle for the chosen geometry was 14 degrees. This gives the minimum pressure drop.

-Combined performance presented in volumetric heat transfer coefficient and performance evaluation criteria were conducted and the results indicate that the volumetric heat transfer coefficient always increases with increasing the pumping power per unit volume.

-All results show heat transfer enhancement over that for the bare model. The maximum enhancement was achieved with a porosity of 25% and at Reynolds number value 2*10^4.

-The Performance Evaluation Criteria are compared with the Reynolds number and correlation was deduced in equation 17

-The best performance is at porosity 25% and Reynolds number 4617.

Nomenclature

HTC	Heat transfer coefficient (W/m^2K)	h_v	Volumetric heat transfer coefficient (W/m^2 K)
T_b	Base temperature of the heat source (°C)	$\dot{m}$	Air mass flow rate (kg/s)
T_{Bulk}	Air bulk temperature at exit (°C)	k_a	Thermal conductivity (W/mK)
$T_{a,i}$	Air inlet temperature (°C)	ε	Porosity
$T_{a,o}$	Air outlet temperature (°C)	Nu	Nusselt number
V	Air velocity (m/s)	Re	Reynolds number
H	Heat source height (mm)	$\dot{Q}$	Heat transfer rate (W)
W	Heat source width (mm)	K	Permeability (m^2)
f	Friction factor	t	Porous insert thickness (mm)
$K_{p,\infty}$	Euler number	V	Gross volume (m^3)
P	Pumping power (W)	PEC	Performance evaluation criteria
ΔP	Pressure drop (Pa)	FEM	finite element method

Subscript

a	Air	o	Outlet
b	Base	v	Volumetric
i	Inlet		

References:

[1]P. Samudre and S. V. Kailas, “Thermal performance enhancement in open-pore metal foam and foam-fin heat sinks for electronics cooling,” Appl Therm Eng, vol. 205, no. November 2021, p. 117885, 2022, doi: 10.1016/j.applthermaleng.2021.117885.

[2]Y. Li, L. Gong, M. Xu, and Y. Joshi, “Hydraulic and thermal performances of metal foam and pin fin hybrid heat sink,” Appl Therm Eng, vol. 166, p. 114665, 2020, doi: 10.1016/j.applthermaleng.2019.114665.

[3]M. Pourramezan, H. Ajam, M. A. Raoufi, and A. Abadeh, “Performance evaluation and optimization of design parameters for twisted conical strip inserts in tubular laminar flow Using

Taguchi approach," International Journal of Thermal Sciences, vol. 152, p. 106324, 2020, doi: 10.1016/j.ijthermalsci.2020.106324.

[4]W. Aboelsoud, W. Wu, L. C. Chow, B. A. Saarloos, and D. P. Rini, "Analysis of thermal and hydraulic performance of V-shape corrugated carbon foam," Int J Heat Mass Transf, vol. 78, pp. 1114–1125, 2014, doi: 10.1016/j.ijheatmasstransfer.2014.07.042.

[5]M. A. Sayed, A. M. T. A. ELdein Hussin, N. A. Mahmoud, and W. Aboelsoud, "Performance evaluation of wire mesh heat exchangers," Appl Therm Eng, vol. 169, no. August 2019, p. 114891, 2020, doi: 10.1016/j.applthermaleng.2019.114891.

[6]S. Mancin, C. Zilio, A. Diani, and L. Rossetto, "Experimental air heat transfer and pressure drop through copper foams," Exp Therm Fluid Sci, vol. 36, pp. 224–232, 2012, doi: 10.1016/j.expthermflusci.2011.09.016.

[7]R. Chein, H. Yang, T. H. Tsai, and C. Lu, "Experimental study of heat sink performance using copper foams fabricated by electroforming," Microsystem Technologies, vol. 16, no. 7, pp. 1157–1164, 2010, doi: 10.1007/s00542-009-0950-y.

[8]S. Y. Kim, J. W. Paek, and B. H. Kang, "Thermal performance of aluminum-foam heat sinks by forced air cooling," IEEE Transactions on Components and Packaging Technologies, vol. 26, no. 1, pp. 262–267, 2003, doi: 10.1109/TCAPT.2003.809540.

[9]S. Y. Kim, J. W. Paek, and B. H. Kang, "Flow and heat transfer correlations for porous fin in a plate-fin heat exchanger," J Heat Transfer, vol. 122, no. 3, pp. 572–578, 2000, doi: 10.1115/1.1287170.

[10]W. Wang, J. Guo, S. Zhang, J. Yang, X. Ding, and X. Zhan, "Numerical study on hydrodynamic characteristics of plate-fin heat exchanger using porous media approach," Comput Chem Eng, vol. 61, pp. 30–37, 2014, doi: 10.1016/j.compchemeng.2013.10.010.

[11]H. E. Ahmed, O. T. Fadhil, and W. A. Salih, "Heat transfer and fluid flow characteristics of tubular channel partially filled with grooved metal foams," International Communications in Heat and Mass Transfer, vol. 108, p. 104336, 2019, doi: 10.1016/j.icheatmasstransfer.2019.104336.

[12]B. Kotresha and N. Gnanasekaran, "Determination of interfacial heat transfer coefficient for the flow assisted mixed convection through brass wire mesh," International Journal of Thermal Sciences, vol. 138, no. April 2018, pp. 98–108, 2019, doi: 10.1016/j.ijthermalsci.2018.12.043.

[13]T. Chen, G. Shu, H. Tian, T. Zhao, H. Zhang, and Z. Zhang, "Performance evaluation of metal-foam baffle exhaust heat exchanger for waste heat recovery," Appl Energy, vol. 266, no. March 2019, p. 114875, 2020, doi: 10.1016/j.apenergy.2020.114875.

[14]S. Kiwan, H. Alwan, and N. Abdelal, "An experimental investigation of the natural convection heat transfer from a vertical cylinder using porous fins," Appl Therm Eng, vol. 179, Oct. 2020, doi: 10.1016/j.applthermaleng.2020.115673.

[15]M. Izadi, "Effects of porous material on transient natural convection heat transfer of nano-fluids inside a triangular chamber," Chin J Chem Eng, vol. 28, no. 5, pp. 1203–1213, May 2020, doi: 10.1016/j.cjche.2020.01.021.

[16]S. Kiwan, "Thermal analysis of natural convection porous fins," Transp Porous Media, vol. 67, no. 1, pp. 17–29, Mar. 2007, doi: 10.1007/s11242-006-0010-3.

[17]M. A. Saada, S. Chikh, and A. Campo, "Natural convection around a horizontal solid cylinder wrapped with a layer of fibrous or porous material," Int J Heat Fluid Flow, vol. 28, no. 3, pp. 483–495, Jun. 2007, doi: 10.1016/j.ijheatfluidflow.2006.05.003.

[18]S. A. M. Mehryan, F. M. Kashkooli, M. Ghalambaz, and A. J. Chamkha, “Free convection of hybrid Al2O3-Cu water nanofluid in a differentially heated porous cavity,” Advanced Powder Technology, vol. 28, no. 9, pp. 2295–2305, Sep. 2017, doi: 10.1016/j.apt.2017.06.011.

[19]M. Nazari, M. Ashouri, M. H. Kayhani, and A. Tamayol, “Experimental study of convective heat transfer of a nanofluid through a pipe filled with metal foam,” International Journal of Thermal Sciences, vol. 88, pp. 33–39, 2015, doi: 10.1016/j.ijthermalsci.2014.08.013.

[20]M. Izadi, M. M. Shahmardan, M. J. Maghrebi, and A. Behzadmehr, “NUMERICAL STUDY OF DEVELOPED LAMINAR MIXED CONVECTION OF Al2O3/WATER NANOFLUID IN AN ANNULUS,” Chem Eng Commun, vol. 200, no. 7, pp. 878–894, Jul. 2013, doi: 10.1080/00986445.2012.723077.

[21]M. Izadi, S. Sinaei, S. A. M. Mehryan, H. F. Oztop, and N. Abu-Hamdeh, “Natural convection of a nanofluid between two eccentric cylinders saturated by porous material: Buongiorno’s two phase model,” Int J Heat Mass Transf, vol. 127, pp. 67–75, Dec. 2018, doi: 10.1016/j.ijheatmasstransfer.2018.07.066.

[22] COMSOL Multiphysics, 5.3 a,COMSOL Inc."

[23] Balaji, C., Hölling, M., & Herwig, H. (2006). Nusselt number correlations for turbulent natural convection flows using asymptotic analysis of the Near-Wall Region. Journal of Heat Transfer, 129(8), 1100–1105. https://doi.org/10.1115/1.2737485